Composites Research

Vol. 32, No. 6, 375-381 (2019)
DOI: http://dx.doi.org/10.7234/composres.2019.32.6.375
ISSN 2288-2103(Print), ISSN 2288-2111(Online)

Paper

Effect of Interface on the Properties of Polyamide 6/Carbon Nanotube Nanocomposites Prepared by In-situ Anionic Ring-opening Polymerization

Jin Hong Min*, Mongyoung Huh, Seok Il Yun*†**

ABSTRACT: Multiwalled carbon nanotubes (MWCNTs) are covalently functionalized with isocyanates by directly reacting commercial hydroxyl functionalized MWCNTs with excess 4,4'-methylenebis (phenyl isocyanate) (MDI) and hexamethylene diisocyanate (HDI). HDI-modified MWCNTs results in a higher surface isocyanate density than MDI-modified MWCNTs. Anionic ring-opening polymerization of ε-caprolactam is conducted using a sodium caprolactam initiator in combination with a di-functional hexamethylene-1,6-dicarbamoylcaprolactam activator in the presence of isocyanate functionalized MWCNTs. This polymerization proceeds in a highly efficient manner at relatively low reaction temperature (150°C) and short reaction times (10 min). During the polymerization, the isocyanate functionalized MWCNTs act not only as reinforcing fillers but also as second activators. Nanocomposites with HDI modified MWCNTs exhibit higher reinforcement and faster isothermal crystallization than MDI modified MWCNTs. The results show that PA6 chains grow more effectively from HDI modified MWCNT surface than from MDI modified MWCNT surface, resulting in stronger interaction between PA6 and MWCNTs.

Key Words: PA6, MWCNT, Isocyanate, Nanocomposite, Anionic ring-opening polymerization

1. INTRODUCTION

Polyamide 6 (PA6) is one of the most widely used engineering plastics due to its superior mechanical and thermal properties, oil resistance, low cost and ease of synthesis [1-3]. These characteristics have usually been utilized to produce filler reinforced PA6 composites in many high-end fields [4,5]. The high melting temperature and viscosity of thermoplastics limits their growth in polymer composites, mainly due to expensive and time-consuming manufacturing processes such as autoclaves or hot presses. Significant reduction in matrix viscosity is important for cost effective production of thermoplastic composites with optimum impregnation of the reinforcements by the matrix. This can be achieved by the reactive processing (or monomer casting) techniques, where the thermoplastic matrices are synthesized in situ, through polymerization of low-viscosity monomers or oligomers in the presence of the reinforcements [6-10]. The most commonly used polymerization types is the ring-opening polymerization of ε-caprolactam (ECL). In this mechanism, ring-shaped monomer molecules are opened and transformed into high molecular weight PA6 without liberation of by-products by means of an activator and a catalyst. The process is carried in a way that the ECL polymerization and PA6 crystallization occur simultaneously at temperatures 40-60°C lower than the melting point of the resulting PA6 (220°C). This significantly reduces the overall production cycle time and increases the energy efficiency of the process. Despite CNTs having desirable physical properties, the full potential of employing carbon nanotubes (CNTs) as reinforcements has been severely limited because of the poor dispersion and poor interfacial bonding of CNTs to monomer or polymer matrices. These problems

Received 9 October 2019, received in revised form 31 October 2019, accepted 9 December 2019

*Department of Chemical Engineering and Materials Science, Sangmyung University, Seoul 03016, Korea
*†Department of Chemical Engineering and Materials Science, Sangmyung University, Seoul 03016, Korea, Corresponding author (E-mail: yunsans@smu.ac.kr)
**Affiliation Korea Institute of Carbon Convergence Technology, Jeonju 54853, Korea

largely stem from the smooth surface of CNTs, which is chemically inert and incompatible with most solvents and polymers [11-13]. Recently, the functionalization of CNTs with PA6 by using the grafting-from strategy has been adopted to improve the dispersion and interfacial bonding of CNTs in PA6 matrix [14,15]. Utilizing di-isocyanate as a surface modifier for hydroxyl functionalized CNT and subsequent CNT surface initiated anionic polymerization of ECL have been a facile route to PA6 functionalization of CNTs [14,15]. In the present study, we used two different modifiers, 4,4'-methylenebis (phenyl isocyanate) (MDI) and hexamethylene diisocyanate (HDI) to incorporate isocyanate functionalities onto the surface of MWCNTs. Anionic ring-opening polymerization of ECL was conducted in the presence of MDI and HDI modified MWCNTs by using a sodium caprolactam (C10) initiator in combination with a di-functional hexamethylene-1,6-dicarbamoylcaprolactam (C20) activator. In this case, the PA6 chain grows from the MWCNT surface, while C10/C20 initiate polymerize in the bulk ECL melt as shown in Fig. 1. To date, no direct comparison between MDI and HDI for preparing isocyanate functionalized CNTs has been reported in the literature. In this study, compared to unmodified CNTs, the isocyanate functionalized CNTs, especially HDI modified CNTS, more effectively reinforced the nanocomposites and accelerate PA6 isothermal crystallization

2. EXPERIMENTAL

2.1 Materials

The ECL used was an anionic polymerization grade (AP-Nylon® grade) supplied by Bruggemann Chemical (Heilbronn, Germany) as it has a low moisture content (<100 ppm). The MDI, HDI, dibutyltin dilaurate (DBDL) and anhydrous tetrahydrofuran (THF) were purchased from Sigma-Aldrich (US). A C20 as an activator and a C10 initiator were purchased from Brueggemann Chemical. MWNTs-OH (3.06 wt% OH) was purchased from US Research Nanomaterials, Inc (purity > 95%, diameter 10-20 nm, length 10-30 μm).

2.2 Surface modification of hydroxyl functionalized MWCNTs

The CNT-OH (2 g) in anhydrous THF (100 mL) was sonicated for 20 min to obtain a homogeneous suspension of CNT-OH, and was then put into a 100 mL three-necked round-bottom flask. After a mechanical stirring under nitrogen (N_2), the mixture was heated to 50°C, followed by addition of 500 mol% MDI (or HDI) relative to CNT-OH and 1.25 mL DBDL catalyst. The reaction was maintained at 50°C for 1 h and filtered and dried.

2.3 In-situ synthesis of PA6/MWNTs Nanocomposite

ECL monomers (100 g) were put into a three-necked flask and heated to 80°C under a nitrogen atmosphere. After the monomer was melted, MDI (or HDI) modified MWCNTs (0-1 wt%) were added. The mixed melt was stirred and sonicated for another 20 min. The C10 (2.5 wt%) and C20 (1.67 wt%) were added to the mixed melt then immediately cast into a mold at 150°C and reacted for 10 min; thus, the product of PA6 nanocomposite was obtained.

2.4 Characterization

Nanocomposite samples were cut into thin flakes and weighed. The samples were refluxed for 24 h to remove unreacted ECL monomer in hot distilled water (95°C). After drying, samples were weighed again. The sample weight difference was used as 100 × (weight after refluxing / weight before refluxing) to obtain a degree of conversion (wt%). Fourier transform infrared (FT-IR) spectra were obtained by use of a Bruker/Tensor27 spectrometer (Germany). The spectrum of samples on the ATR plate was collected at a 4 cm^{-1} resolution with 2 min intervals by co-adding 16 scans. The isothermal crystallization of PA6 and PA6 nanocomposites was studied by differential scanning calorimetric (DSC) analysis with a modulated DSC (Q200, TA instruments, US). The samples of about 10 mg were heated quickly from ambient temperature to 250°C under nitrogen atmosphere, and then held for 5 min to eliminate the effect of the previous thermal history. Then the samples were quenched to isothermal crystallization temperature (188, 190, and 192°C), and the isothermal crystallization was carried out at these temperatures

3. RESULTS AND DISCUSSION

The MWCNT-OH material was reacted with MDI and HDI to produce isocyanate functionalized MWCNTs (Fig. 1).

Fig. 2 shows the FTIR spectra of MWCNT-OH, isocyanate functionalized MWCNTs by MDI and HDI. Unlike the MWCNT-OH, addition of excess TDI and MDI to the MWCNT-OH, resulted in the appearance of clearly discernable bands at 2360 and 2337 cm^{-1} corresponding to C=O bond and asymmetric stretching of the appended terminal isocya-

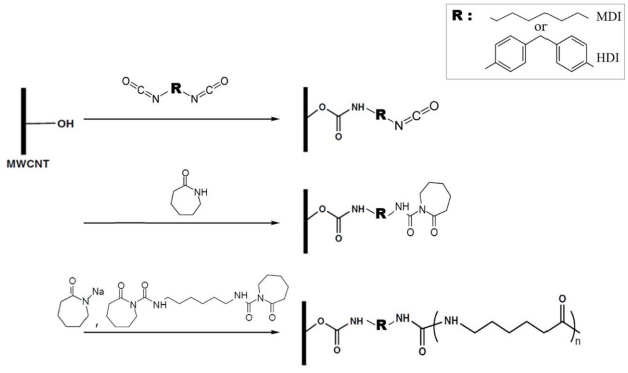

Fig. 1. Synthesis of isocyanate functionalized MWCNTs and subsequent PA6 chain growth from functionalized MWCNTs

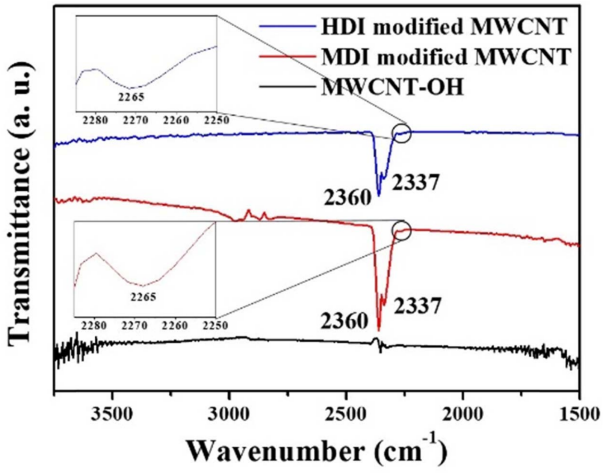

Fig. 2. FTIR spectra of the MWCNT-OH, MDI and HDI-modified MWCNT

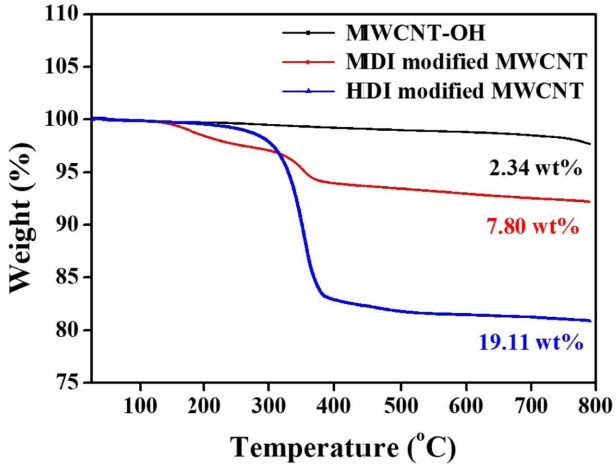

Fig. 3. TGA data for the MWCNT-OH, MDI and HDI-modified MWCNT

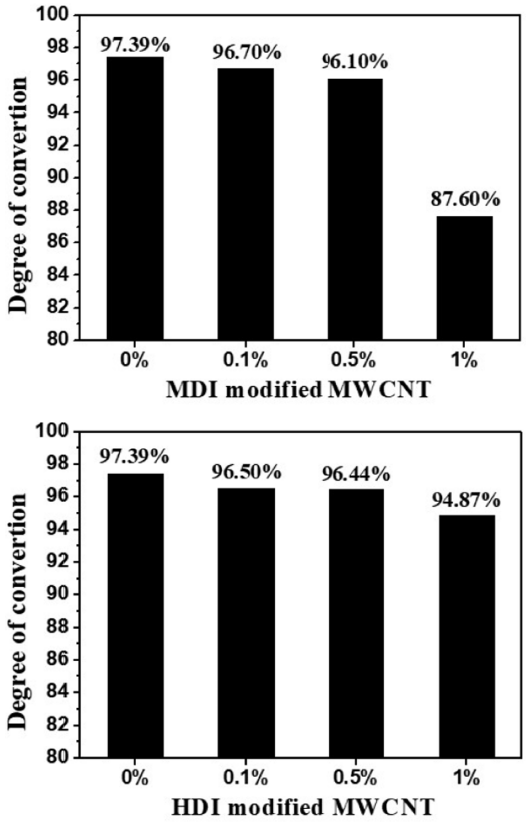

Fig. 4. The effect of MWCNTs on the degree of conversion

nate groups, respectively [16]. The typical band at 2265 for isocyanate group was also observed [14,15]. The results indicate that the isocyanates were successfully incorporated into the surface of MWCNT-OH using the coupling agents, HDI and MDI. To gain a more quantitative picture of the extent of nanotube functionalization, TGA analysis was performed on the surface functionalized MWCNTs as depicted in Fig. 3. For comparison, the TGA plot of MWCNT-OH showed a gradual mass loss of around 2.34 wt% as the temperature reaches 800°C. There is a distinct difference in mass loss region between 300 and 400°C for different isocyanate functionalized MWCNTs. HDI modified MWCNTs showed much greater loss than MDI modified MWNTs. The mass loss was found to be 7.80 and 19.11 wt%, for the MDI and HDI modified MWCNT, respectively. Considering that the starting nanotubes have a hydroxyl group concentration of 3.06 wt%, the TGA results indicate that about 55.4% of the available hydroxyl groups reacted with HDI despite the poor solubility of MWCNTs in THF. However, for MDI modified MWNTs, only a 12.% of available OH groups reacted with MDI.

In the presence of isocyanate functionalized MWCNTs, anionic ring-opening polymerization of ECL was conducted by using a C10 initiator in combination with a C20 activator. Isocyanate groups of MDI and HDI modified MWCNTs could serve as activators of ECL during the in situ polymerization. In this case, Polymerization occurs from the MWCT surfaces and in bulk ECL melts by C10, simultaneously. Modified or unmodified MWCNTs were found to be well dispersed in the molten ECL by visual inspection. The molten ECL and final composite containing MWCNTs showed no difference with respect to CNT dispersion by CNT surface modification [17]. The effects of the MWCNT concentration on the degree of conversion are presented in Fig. 4. The final degree of conversion showed the downward trend with increasing MWCNT concentration. According to the TGA results, compared to HDI modified MWCNTs, MDI modified MWCNTs contain more unreacted OH functionalities that can terminate the anionic ring-opening polymerization, resulting in the greater reduction in conversion for nanocomposites.

The tensile test results of neat PA6 and PA6/MWCNTs nanocomposites with different CNT loadings are summarized in Fig. 5. Nanocomposites with HDI-modified CNTs showed higher mechanical improvement than MDI-modified CNTs

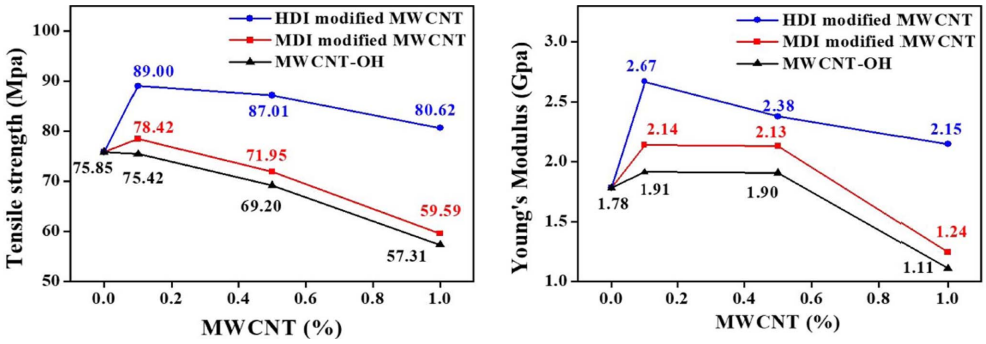

Fig. 5. Effect of MWCNT loading on the mechanical properties of PA6/MWCNT nanocomposites, (a) the tensile strength and (b) Young's modulus

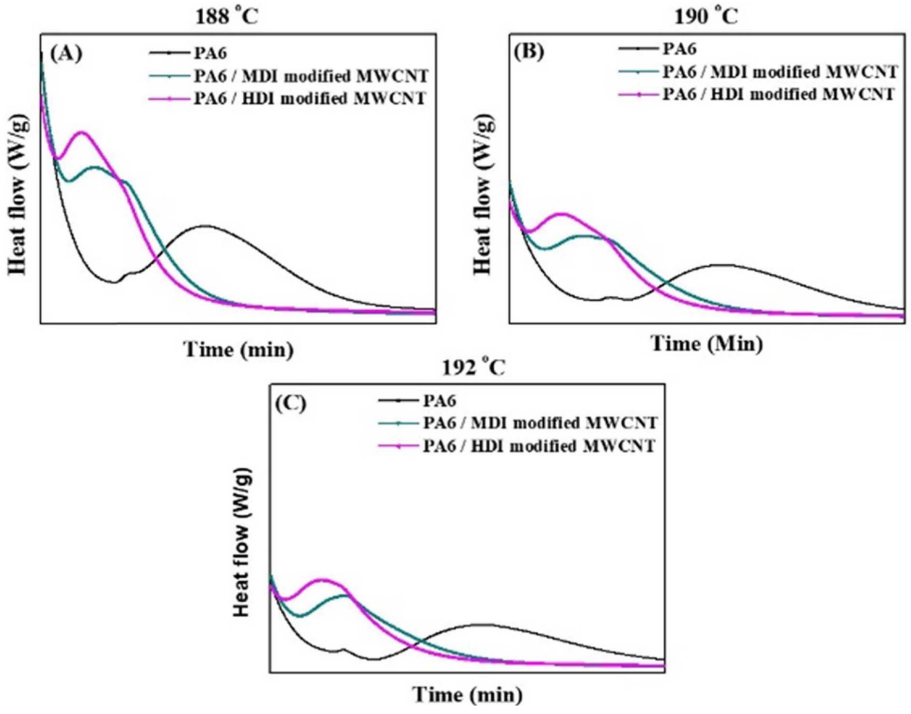

Fig. 6. DSC thermograms (cooling scan) of PA6 and PA6/MWCNT nanocomposites at various T_c at (a) 188 (b) 190 and (c) 192°C

and hydroxyl CNTs. The results clearly displayed that higher isocyanate density on the CNT surface led to higher PA6 grafting density during the polymerization. High PA6 grafting density of CNT resulted in stronger interactions and better compatibility between PA6 and MWCNT which are responsible for higher mechanical reinforcement of nanocomposite compared to lower isocyanate density on the CNT surface (MDI modified MWCNT).

In order to study the isothermal crystallization kinetics, the heat release during the process was monitored. Fig. 6a-c shows the characteristic isothermal crystallization exotherms of PA6 and PA6 nanocomposites containing surface modified CNTs with CNT content of 0.1%. From the Fig. 6, the relative degree of crystallinity, $X(t)$ at time t, can be established by

$$X(t) = \frac{\int_0^t \left(\frac{dH}{dt}\right) dt}{\int_0^\infty \left(\frac{dH}{dt}\right) dt} \quad (1)$$

where the denominator is the total area under the isothermal crystallization graph by DSC. Fig. 7 shows $X(t)$ as a function of the crystallization time t at different crystallization temperatures. A typical sigmoidal evolution is seen in all three curves. From these Fig. 7, it can be concluded that the addition of CNTs significantly shortened the corresponding crystallization time of PA6. One of the most important rate parameter, crystallization half-time ($t_{0.5}$) which is defined as the time taken the relative crystallinity of the sample reaches the value of 50% can be directly obtained from Fig. 7.

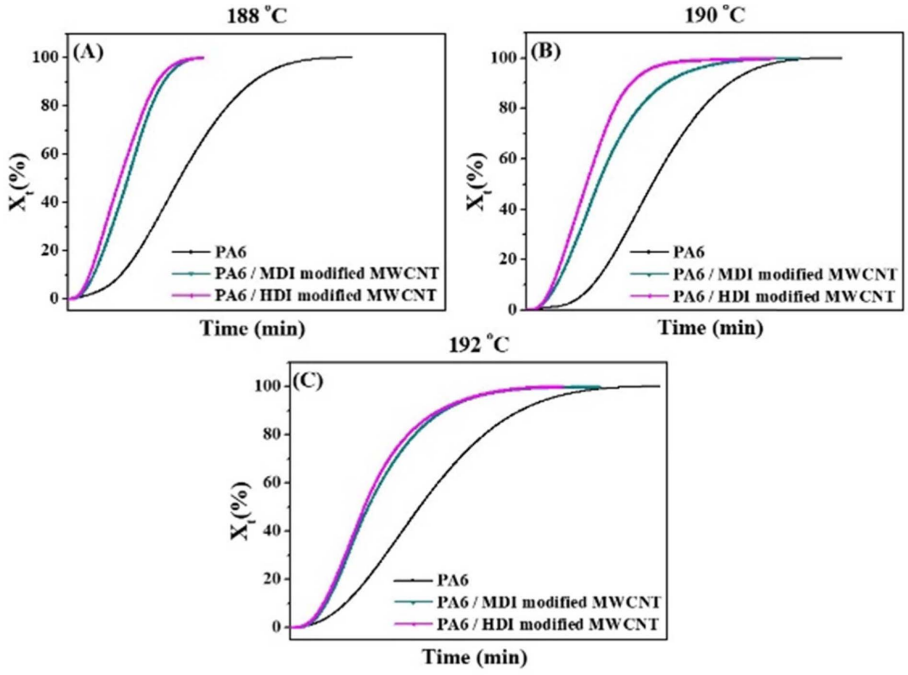

Fig. 7. Effect of surface modification on the relative degree of crystallinity, $X(t)$ at different T_c

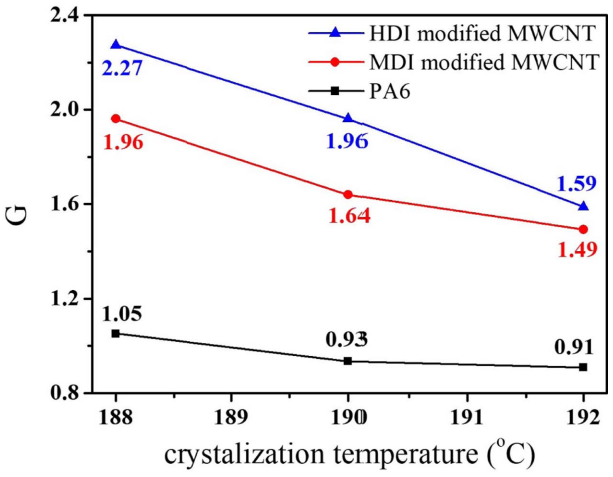

Fig. 8. The variation of G value (=1/$t_{0.5}$) as a function of T_c for PA6 and PA6/MWCNT nanocomposites

The reciprocal (G) of $t_{0.5}$ is usually used as the overall crystallization rate and G values at different crystallization temperature of 188, 190, 192°C were summarized in Fig. 8. At all T_c, the G value of the nanocomposites was greater than neat PA6 indicating that CNT acted as a nucleating agent for PA6. Particularly, the HDI modified MWCNT accelerated PA6 crystallization more efficiently than the MDI modified MWCNT. The high surface PA6 density of CNTs may have resulted in stronger interfacial interactions and compatibility of nanocomposite, than the low PA6 density of CNT surfaces. The enhanced compatibility and interfacial interactions between filler and matrices generally accelerates the nucleation of crystallization very effectively. In addition, for all the samples the G value increased with T_c, in agreement with the kinetics theory of crystallization, which expects for crystallization close to the melting temperature, a decrease of undercooling will slow the crystallization with increasing T_c. The isothermal melt crystallization kinetics of the samples was further analyzed by the well-known Avrami equation, which assumes the relative degree of crystallinity (X_t) develops with crystallization time (t) as follows [18]:

$$X(t) = 1 - \exp(-kt^n) \tag{2}$$

or

$$\ln[-\ln(1-X(t))] = \ln k + n\ln t \tag{3}$$

where n is Avrami exponent which depends on the mechanism of nucleation and growth of the crystal and k is the overall crystallization rate constant. Plotting $\ln[-\ln(1 - X(t)]$ versus $\ln t$ therefore yields a straight line with a slope of n, and the k value can be determined from the point of intersection with the y axis.

Fig. 9 shows the linear relation between $\ln[-\ln(1 - X(t)]$ and $\ln t$ for the samples at various T_c. Table 1 summarizes the values of n and k for neat PA6 and its nanocomposites crystallized at different T_c. The k values for the nanocomposites found to be greater than those for neat PA6 and nanocomposites with HDI-modified CNTs which is consistent with G

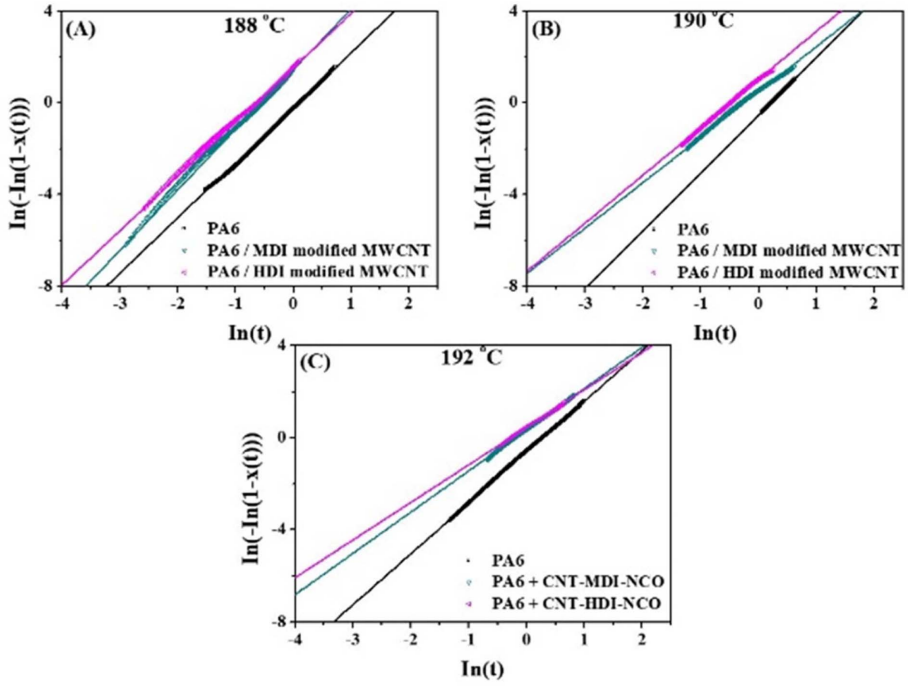

Fig. 9. The linear relation of ln[-ln(1 - *X*(*t*)] and ln *t* for PA6 and PA6/MWCNT nanocomposites at various T_c at (a) 188 (b) 190 and (c) 192°C

Table 1. Isothermal melt crystallization kinetic parameters for PA6 and MWCNT nanocomposites

Sample	T_c (°C)	n	K (min^{-n})	t 1/2 (min)[a]	t 1/2 (min)[b]
PA6	188	2.40	0.82	0.93	0.95
	190	2.38	0.58	1.08	1.07
	192	2.21	0.54	1.12	1.10
MDI modified MWCNT	188	2.63	2.63	0.50	0.51
	190	1.97	1.97	0.65	0.61
	192	1.79	1.79	0.67	0.67
HDI modified MWCNT	188	2.41	2.41	0.45	0.44
	190	2.09	2.09	0.51	0.51
	192	1.63	1.63	0.60	0.63

[a] Determined from Fig. 7
[b] Calculated eq. (4)

values. As anticipated the *k* values also decreased with increasing T_c. The Avrami exponent (*n*) represents the dimensionality of the growth, three-dimensional crystallization a theoretical value of 3 should be obtained for *n*. The lower-than-3 n values in the table could be due to mixed 3D and 2D crystallization. For T_c = 188°C, the *n* values were found to be 2.4~2.7 and almost unchanged with the addition of CNTs, suggesting that despite the CNT loading, the crystallization mechanism of PA6 remained unchanged. However, at the higher T_c = 190 and 192°C, *n* values decreased to 2.21 for PA6. Compared to PA6, the *n* values were dropped further to 1.63 for nanocomposites with increasing T_c. The changes in Avrami exponent after the addition of MWCNTs indicate that the presence of MWCNT modified the growth pattern of PA6 crystals. With $X(t)$ = 0.5, from eq. (3) the relation between the half-time and the crystallization parameter *k* can be expressed as

$$t_{0.5} = \left(\frac{\ln 2}{k}\right)^{1/n} \tag{4}$$

The half-time can be directly determined from X(t) data (Fig. 7) or be calculated using eq. (4). Usually, the Avrami equation can fit data in the primary crystallization range Nevertheless a comparison between the experimental and the theoretically predicted values of the half-crystallization time also indicates that the fits are very good up to 50% conversion since the values are quite similar.

4. CONCLUSIONS

The isocyanate functionalized MWCNTs was prepared by directly reacting commercial hydroxyl functionalized MWCNTs with excess MDI and HDI. HDI-modified MWCNTs resulted in the CNTs with higher isocyanate density than MDI-modified MWCNTs. Anionic ring-opening polymerization of ECL was conducted by using a C10 initiator in combination with a C20 activator in the presence of isocyanate functionalized CNTs as the second activator and reinforcing filler. This polymerization proceeded in a highly efficient manner at relatively low reaction temperature (150°C) and short reaction times (10 min). The isocyanate functionalized CNTs improved

nanocomposites more effectively than hydroxyl functionalized CNTs. The results indicate that PA6 was successfully grown from the MWCNT surface during the polymerization in the ε-caprolactam melt. Nanocomposites with HDI modified MWCNTs showed higher reinforcement and faster isothermal crystallization than MDI modified MWCNTs. The results showed that PA6 chains grew more effectively from HDI modified MWCNTs than from MDI modified MWCNTs, resulting in stronger interaction between PA6 and MWCNT surface.

ACKNOWLEDGEMENT

For financial support of this research, we thank the core technology development program (10052724) funded by the Ministry of Trade, Industry & Energy (Republic of Korea).

REFERENCES

1. Marchildon, K., "Polyamides - Still Strong After Seventy Years," *Macromolecular Reaction Engineering*, Vol. 5, 2011, pp. 22-54.
2. Pervaiz, M., Faruq, M., Jawaid, M., and Sain, M., "Polyamides: Developments and Applications Towards Next-Generation Engineered Plastics," *Current Organic Synthesis*, Vol. 14, 2017, pp. 146-155.
3. Winnacker, M., "Polyamides and Their Functionalization: Recent Concepts for Their Applications as Biomaterials," *Biomaterial Science*, Vol. 5, 2017, pp. 1230-1235.
4. Feldman, D., "Polyamide Nanocomposites," *Journal of Macromolecular Science, Part A-Pure and Applied Chemistry*, Vol. 54, 2017, pp. 255-262.
5. Faridirad, F., Ahmadi, S., and Barmar, M., "Polyamide/Carbon Nanoparticles Nanocomposites: A Review", *Polymer Engineering and Science*, Vol. 57, 2017, pp. 475-494.
6. van Rijswijk, K., Teuwen, J.J.E., Bersee, H.E.N., and Beukers, A., "Textile Fiber-reinforced Anionic Polyamide-6 Composites. Part I: The Vacuum Infusion Process", *Composites Part A-Applied Science and Manufacturing*, Vol. 40, 2009, pp. 1-10.
7. van Rijswijk, K., van Geenen, A.A., and Bersee, H.E.N., "Textile Fiber-reinforced Anionic Polyamide-6 Composites. Part II: Investigation on Interfacial Bond Formation by Short Beam Shear Test", *Composites Part A-Applied Science and Manufacturing*. Vol. 40, 2009, pp. 1033-1043.
8. Barhoumi, N., Maazouz, A., Jaziri, M., and Abdelhedi, R., "Polyamide from Lactams by Reactive Rotational Molding via Anionic Ring-opening Polymerization; Optimization of Processing Parameters", *Express Polymer Letters*, Vol. 7, 2013, pp. 76-87.
9. Vicard, C., De Almeida, O., Cantarel, A., and Bernhart, G., "Experimental Study of Polymerization and Crystallization Kinetics of Polyamide 6 Obtained by Anionic Ring Opening Polymerization of Epsilon-caprolactam", *Polymer*, Vol. 132, 2017, pp. 88-97.
10. Maazouz, A., Lamnawar, K., and Dkier, M., "Chemorheological Study and In-situ Monitoring of PA6 Anionic-ring Polymerization for RTM Processing Control", *Composites Part A-Applied Science and Manufacturing*, Vol. 107, 2018, pp. 235-247.
11. Ajayan P.M., and Tour, J.M., "Nanotube Composites", *Nature*, Vol. 447, 2007, pp. 1066-1068.
12. Sahoo, N.G., Rana, S., Cho, J.W., Li, L., and Chan, S.H., "Polymer Nanocomposites Based on Functionalized Carbon Nanotubes", *Progress in Polymer Science*, Vol. 35, 2010, pp. 837-867.
13. Spitalsky, Z., Tasis, D., Papagelis, K., and Galiotis, C., "Carbon Nanotube-polymer Composites: Chemistry, Processing, Mechanical and Electrical Properties", *Progress in Polymer Science Sci.*, Vol. 35, 2010, pp. 357-401.
14. Yang, M., Gao, Y., Li, H., and Adronov, A., "Functionalization of Multiwalled Carbon Nanotubes with Polyamide 6 by Anionic Ring-opening Polymerization", *Carbon*, Vol. 45, 2007, pp. 2327-2333.
15. Yan, D., and Yang, G., "Synthesis and Properties of Homogeneously Dispersed Polyamide 6/MWNTs Nanocomposites via Simultaneous *in situ* Anionic Ring-opening Polymerization and Compatibilization", *Journal of Applied Polymer Science*, Vol. 112, 2009, pp. 3620-3626.
16. Oumi, L., Mirzaei, M., Ashtari, P., Ramazani, A., Rahimi, M., and Bolourinovin, F., "Isocyanate Functionalized Multiwalled Carbon Nanotubes for Separation of Lead from Cyclotron Production of thallium-201", *Journal of Radioanalytical and Nuclear Chemistry*, Vol. 310, 2016, pp. 633-643.
17. Bernat, P., Hladka, O., Fismanova, M., Roda, J., and Brozek, J., "Polymerization of Lactams. 98: Influence of Water on Thenon-activated Polymerization ε-caprolactam", *European Polymer Journal*, Vol. 44, 2008, pp. 32-41.
18. Avrami, M., "Granulation, Phase Change, and Microstructure Kinetics of Phase Change. III", *The Journal of Chemical Physics*, Vol. 9, 1941, pp. 177-183.